Author/s:
Li, X;Kevin, K;Lam, WK;Ooi, A;Zachreson, C;Geard, N;Tsigaras, L;Bates, S;McGain, F;Morawska, L;Kainer, M;Monty, J

Title:
Mitigating Airborne Infection Transmission in the Common Area of Inpatient Wards—A Case Study

Date:
2025-10-01

Citation:
Li, X., Kevin, K., Lam, W. K., Ooi, A., Zachreson, C., Geard, N., Tsigaras, L., Bates, S., McGain, F., Morawska, L., Kainer, M. & Monty, J. (2025). Mitigating Airborne Infection Transmission in the Common Area of Inpatient Wards—A Case Study. Fluids, 10 (10), pp.267-267. https://doi.org/10.3390/fluids10100267.

Persistent Link:
https://hdl.handle.net/11343/369424

fluids

MDPI

Article

Mitigating Airborne Infection Transmission in the Common Area of Inpatient Wards—A Case Study

Xiangdong Li [1,2,*], Kevin Kevin [1,2], Wai Kit Lam [2], Andrew Ooi [2], Cameron Zachreson [3], Nicholas Geard [3], Loukas Tsigaras [2], Samantha Bates [4,5], Forbes McGain [4,5], Lidia Morawska [1,6], Marion Kainer [4] and Jason Monty [1,2]

1 ARC Training Centre for Advanced Building Systems Against Airborne Infection Transmission (Thrive), Brisbane, QLD 4000, Australia; kevin.kevin@unimelb.edu.au (K.K.); l.morawska@qut.edu.au (L.M.); montyjp@unimelb.edu.au (J.M.)
2 Department of Mechanical Engineering, University of Melbourne, Parkville, VIC 3010, Australia; waikit.lam1@unimelb.edu.au (W.K.L.); a.ooi@unimelb.edu.au (A.O.); loukas.tsigaras@unimelb.edu.au (L.T.)
3 Department of Computing and Information, University of Melbourne, Parkville, VIC 3010, Australia; cameron.zachreson@unimelb.edu.au (C.Z.); nicholas.geard@unimelb.edu.au (N.G.)
4 Western Health, St. Albans, VIC 3021, Australia; samantha.bates@wh.org.au (S.B.); forbes.mcgain@wh.org.au (F.M.); marion.kainer@wh.org.au (M.K.)
5 Department of Critical Care, University of Melbourne, Parkville, VIC 3010, Australia
6 School of Earth and Atmospheric Sciences, Queensland University of Technology, Brisbane, QLD 4000, Australia
* Correspondence: xiangdong.li.1@unimelb.edu.au

Abstract

In a hospital ward, transmission of airborne pathogens can occur in any area where people breathe the same air. These areas include patient rooms and specialised treatment rooms, as well as corridors and common areas. Numerous studies have been conducted to investigate the risk of airborne transmission within hospital rooms where patient care activities take place; however, studies assessing the risk of exposure to airborne pathogens in common areas such as nurse stations and corridors, in which healthcare workers spend up to 63% of their time, are very rare. In this study, we addressed this gap by simulating aerosol transport in the common area of a real inpatient ward encompassing different types of patient rooms and equipped with a mixing ventilation system. The risk of airborne transmission of COVID-19 in the ward was evaluated using a spatially resolved risk model, coupled with the clinical and pathological data on SARS-CoV-2 infection. The results showed that the central-return ventilation system causes directional air flows in the corridors, which enhanced long-distance aerosol transport and were conducive to infection transmission between different rooms. An improved ventilation system was proposed that aimed to reduce air mixing and minimise directional air flows. The improvement involved only rearrangement of air supply and exhaust vents, but led to significant reductions in both particle residence time and travelling distance within the ward, contributing to a nearly two-fold increase and 60% decrease in the areas of low-risk and high-risk zones, respectively, resulting in a 34% reduction in the overall infection probability in the studied area. This study demonstrated the potential of preventing hospital-acquired infection (HAI) via engineering controls and provided recommendations for future studies to assess novel ventilation configurations to reduce transmission risk.

Keywords: hospital wards; ventilation setup; aerosol transport; infection probability; mitigation

Academic Editors: Filiberto Hueyotl-Zahuantitla and Zheng-Tong Xie

Received: 8 September 2025
Revised: 30 September 2025
Accepted: 12 October 2025
Published: 14 October 2025

Citation: Li, X.; Kevin, K.; Lam, W.K.; Ooi, A.; Zachreson, C.; Geard, N.; Tsigaras, L.; Bates, S.; McGain, F.; Morawska, L.; et al. Mitigating Airborne Infection Transmission in the Common Area of Inpatient Wards—A Case Study. *Fluids* **2025**, *10*, 267. https://doi.org/10.3390/fluids10100267

1. Introduction

Hospital-acquired infection (HAI), also known as healthcare-associated infection, is an infection developed in a hospital or other healthcare environment. HAI is one of the most common complications affecting hospital patients, significantly increasing morbidity and mortality. In Australia, more than 170,000 adults contracted HAIs in 2021, resulting in 7583 deaths [1], making HAI the fifth leading cause of deaths in acute care hospitals. HAIs are estimated to account for 2 million hospital bed days in Australia per year, amounting to over 1 billion dollars in annual economic burden [2].

HAIs can occur via multiple transmission routes, among which airborne transmission [3] is an important contributor. Historically, airborne infection transmission has caused many hospital outbreak events, including nosocomial infections of influenza [4], measles [5], tuberculosis [6], chickenpox [7], severe acute respiratory syndrome (SARS) [8], and Middle East respiratory syndrome (MERS) [9]. During the COVID-19 pandemic, airborne infection transmission was the most important cause of HAIs [10], adversely affecting patient treatment and recovery, and putting frontline healthcare workers at risk. Many hospital outbreaks were reported during the COVID-19 pandemic, forcing hospital wards to be closed and healthcare workers to be quarantined [11].

An airborne infection transmission occurs when a susceptible person inhales a certain amount of infectious respiratory particles. In a healthcare setting, the infectious respiratory particles are typically aerosols exhaled by a patient or infected healthcare worker, or pathogen-carrying particles resuspended from a contaminated surface. A thorough understanding of the mechanisms of airborne transmission is crucial to the development of effective prevention strategies. It took some time in the early pandemic phase to reach global consensus that airborne mechanisms were the principal mode of COVID-19 transmission [12]. As a result of early misunderstanding, inappropriate mitigation methods led to numerous nosocomial outbreaks. Since the adoption of airborne protection measures such as enhanced ventilation, air scrubbers, and personal protective equipment (PPE), significant reductions in COVID-related HAIs have been reported [13,14]. However, some studies [13,14] reported that anti-COVID measures have shown varying efficacy in preventing HAIs, which emphasised the need for multidisciplinary and context-specific strategies.

During the COVID-19 pandemic, enhanced mechanical ventilation was one of the key prevention strategies rolled out by Australian hospitals to minimise airborne HAI transmission. In our early field tests in one inpatient ward in Melbourne, Australia [15], the ventilation rate in general patient rooms was between 12 and 25 air changes per hour (ACH), well in excess of the recommended ventilation rate of 6 ACH for Class S rooms [16] and even exceeding that in negative pressure isolation rooms. Such high ventilation rates are undoubtedly helpful for diluting and removing infectious aerosols in the air. However, the high energy consumption associated with enhanced mechanical ventilation in healthcare settings has become a major concern, with many urging for more sustainable mitigation strategies [12,17]. Although the World Health Organization (WHO) has declared the end of the COVID-19 pandemic, airborne infection transmission remains a major threat to public health. Developing sustainable prevention strategies is still of great importance in the post-pandemic era.

Engineering controls have shown the potentials to mitigate airborne transmission in hospital wards by mechanically removing infectious aerosols from the air [18]. Because airborne respiratory particles are very small (less than 1 μm in diameter on average [19]), their movement in indoor spaces is dominated by the air flow. Theoretically, airborne transmission can be mitigated by optimally organising airflow in terms of pressure, direction, and velocity to ensure that airborne respiratory particles are rapidly removed from

the environment. However, airflow patterns in hospital wards are highly complicated and dynamic. The main reason is that the configuration and layout of patient and staff rooms in a hospital ward varies with the ward's design and purpose [20]. Various types of rooms are often arranged in a single ward and rooms with different functions have different ventilation requirements and/or designs. The arrangement of different rooms has a profound impact on the ward's overall air flow pattern and effectiveness of HAI prevention [21].

However, existing studies on aerosol transport in healthcare settings have largely focused on individual hospital rooms, including operating rooms [22], outpatient clinic rooms [23], and negative pressure isolation rooms [24]. Limited studies have investigated the effects of human and door movement on aerosol transport across adjacent rooms [25]. Air flow and aerosol transport in a complete ward, especially in the common areas (e.g., corridors, nurse stations, staff lounge, and other shared spaces), has rarely been investigated. This is a crucial oversight in relation to HAIs among healthcare workers because these workers spend substantial amounts of time (up to 63% [26,27]) in common areas around the ward such as corridors, nurse stations, and break rooms. In particular, corridors connect patient rooms and are frequently accessed by healthcare workers, patients, and visitors. In common areas, HAI transmission may occur between people in close proximity or through long-range transmission mediated by cross-corridor air flows and human movement between areas [28]. An effective prevention strategy against airborne infection transmission must not only control the infection risks within individual rooms, but also minimise the transport of aerosols between the common area and various rooms.

Developing context-specific HAI prevention strategies requires an in-depth understanding of the overall air flow field and aerosol transport in the common area subjected to the ward's physical configuration and ventilation setup. As a demonstration, this study analysed the air flow and aerosol distribution in a real hospital ward in Melbourne, Australia, with the aim of quantifying the associated airborne transmission risks. In Section 2, computational fluid dynamics (CFD) was employed to simulate and visualise the air flow field and aerosol distribution, based on which a spatially resolved risk model [29] was used to quantify the airborne infection risk in the ward. In Section 3, an improved ventilation design was tested and compared to the current ventilation setup, demonstrating the great potentials of engineering controls for HAI prevention. Conclusions were given in Section 4 alongside recommendations for future work.

2. HAI Risk in the Hospital Ward

2.1. AIR Flow Field and Aerosol Transport in the Ward

We investigated an inpatient ward that predominantly treats patients with respiratory illnesses, including transmissible infective respiratory diseases, as well as providing general medicine care. The floorplan of the ward is shown in Figure 1. The ward had a floor area of 1180 m^2 and a net floor height of 2.7 m. It encompassed eight single-bed negative pressure isolation (Class N) rooms (magenta rooms in the figure), 11 double-bed general patient rooms (white rooms), and two single-bed acute care rooms (pink rooms), as well as three nurse stations (NS-1 to NS-3 in the figure), a staff lounge, and several work rooms (azure rooms). Both the general patient and acute care rooms were standard pressure rooms (Class S, room number S01 to S13).

The pressure in the rooms was controlled following the guidelines published by the Victorian Health and Human Services Building Authority [15]. The pressure was maintained at −30 Pa in the Class N patient rooms and −15 Pa in their anterooms relative to the corridor. The doors to the Class N rooms were well sealed. Pressure stabilisers were installed in the walls leading to each anteroom (Figure 1). The air passage size

of the pressure stabilisers was automatically adjustable, with a mean passage size of 600 mm × 20 mm according to on-site measurement.

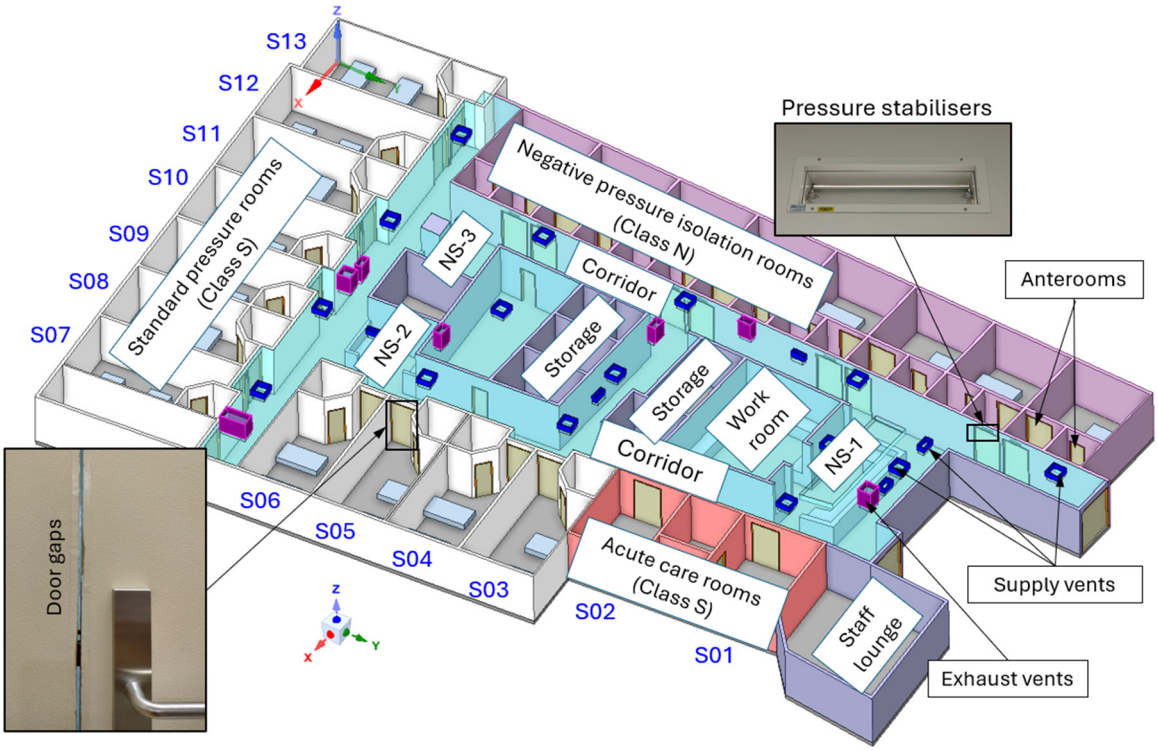

Figure 1. The floorplan of the investigated inpatient ward.

A small positive pressure (~1.0 Pa) was measured in the Class S rooms relative to the corridor when the doors were closed. As there were no air exhaust vents in the rooms, and the exhaust fans in the toilets could only discharge a small proportion of the supplied air, directional airflows were formed from the rooms into the corridor. When the doors were closed, air mainly leaked through the door gaps. For each door of the Class S rooms, a vertical gap with the door height (2140 mm) and a horizontal gap with the door width (1400 mm) were observed, as shown in Figure 1. The width of the gaps was 8 mm on average, making the gaps account for 0.95% of the total door area.

The common area, including the corridors, nurse stations (NS-1 to NS-3), and work rooms, was equipped with a mixing ventilation system, where air was supplied through diffusers and exhausted via grilles mounted in the ceiling. Our field test under normal operating conditions found a total air supply rate of 1555 L/s into the studied common area and a total exhaust rate of 1974 L/s out of this area, respectively. The differential flow rate of 419 L/s was mainly due to the aforementioned excess supply of air from Class S rooms via the door gaps.

The space occupied by air in the common area was extracted as the domain of CFD simulations, as illustrated by the semi-transparent light blue space in Figure 1. The patient rooms, storage rooms, and lounge room were not included in the simulations. Instead, air and aerosol leakage into or out of the common area is accounted for via boundary conditions at the pressure stabilisers and door gaps. The domain was discretised using tetrahedral cells with refined prism cells in the near-wall regions. Mesh independence was achieved at 9.8 million cells as a further mesh refinement using a factor of 1.3 in all coordinate directions (resulting in a total cell count of 18.6 million) only caused a small change of less than 0.5% in the velocity profile along a 35 m horizontal line along the corridor. The air flow is modelled using the Reynolds averaged Navier–Stokes (RANS)

equations coupled with the SST k-ω model for air turbulence. The transport of aerosol is modelled using the Lagrangian method. Details of the above models, numerical procedures, and validations have been discussed elsewhere [30,31] and will not be repeated here.

The boundary conditions of the domain were specified according to field measurements, as listed in Table 1. It should be noted that the flow rates via the supply and exhaust vents used in the computations were based on our field tests in the ward. The flow rates were found to be unevenly distributed over all vents. For example, the supply rate via the diffusers were 17–107 L/s, resulting in supply velocities 0.12–0.58 m/s at the supply diffusers. Volume flow rates were specified at the exhaust vents. In order to balance the overall mass flow rate, a negative pressure of −10.0 Pa was specified at the pressure stabilisers leading to the Class N rooms. The turbulence quantities including turbulent kinetic energy k and specific turbulence dissipation rate ω at all inlets were estimated based on their hydrodynamic diameters. Particles are assumed to be evenly injected into the corridor via the door gaps of the Class S rooms. Although human exhaled respiratory particles are distributed in a wide size range, this study was focused on the airborne part given the door gaps were far from the patient bed. A uniform diameter of 1.0 µm was used for the airborne particles according to the experimental measurement of Morawska et al. [19] and mass fraction of 1.0×10^{-13} at the door gaps according to a previous calculation [29]. The simulations were performed using the commercial CFD code Ansys CFX 2024R1. Convergence was achieved within 5000 iterations when the residual of all equations dropped below 10^{-4}.

Table 1. CFD boundary conditions based on field test.

Supply vents	Total number of vents	23
	Total area (m^2)	6.66
	Total supply rate (L/s)	1555
	Supply from single vent (L/s)	17–107
Exhaust vents	Total number of vents	7
	Total area (m^2)	2.16
	Total exhaust rate (L/s)	1874
	Exhaust via single vent (L/s)	25–1002
Door gaps	Total number of gaps	13
	Total area (m^2)	0.473
	Total exhaust (L/s)	419
	Exhaust via each vent (L/s)	36.4
	Particle mass fraction	1.0×10^{-13}
Pressure stabilisers	Pressure	−3.0 Pa

Figure 2 shows the simulated air flow field in the horizontal plane at the height of 1.2 m from the floor (Z = 1.2 m) representing the typical breathing plane of seated occupants [32]. The air flow in the common area was, for the most part, evenly distributed. Relatively high speed was only observed under the supply vents and next to the door gaps of the Class S rooms. Overall, air flowed in the +Y direction in the corridors because a large return vent existed at the end of the corridor. At the low-Y end, highly complicated flows were observed in some local regions. The current ventilation setup only had a small number of exhaust vents, which were unevenly distributed and generated different local discharge rates across the common area. Similar "corridor-return" or "central-return" ventilation schemes are extensively used in many hospital wards due to their simplicity and low capital cost. However, as shown in Figure 2, they resulted in directional air flows and enhanced air mixing, and were likely to be the main cause of cross-corridor and long-distance airborne infection transmissions [28,33].

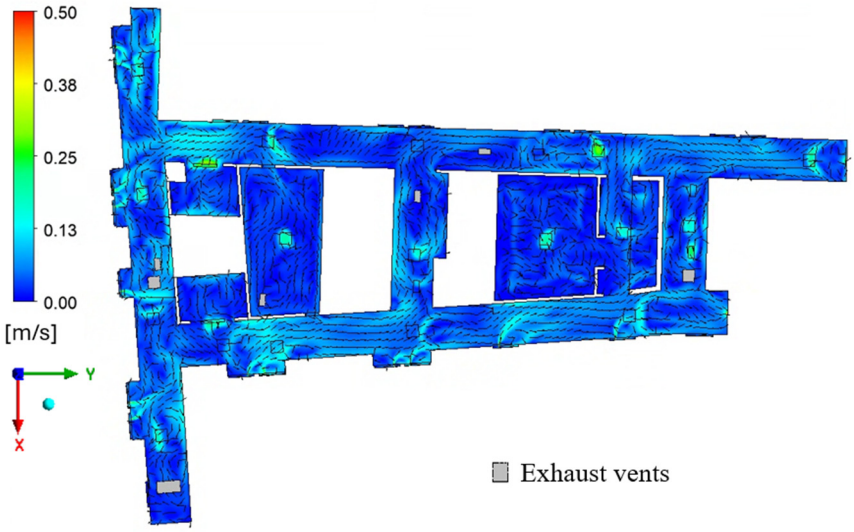

Figure 2. Overall air flow field at Z = 1.2 m.

For particle simulation, the maximum particle tracking time was 2 h, which was long enough to account for most particle trajectories in the domain. It was assumed that the particles settle on solid surfaces as soon as they collided with the surfaces [30]. The simulated aerosol distribution pattern in the common area is shown in Figure 3. The results showed that the particles had a mean residence time of 255 s. A few particles had a longer residence time larger than 30 min, indicating that these particles were trapped in vortex flows and remained airborne for a prolonged period. The particles were transported into most regions of the common area except in the work room behind nurse station NS-1, which did not have an air exhaust, thus only allowed air to flow out. As expected, high aerosol concentration was found mainly in the corridors next to the Class S rooms from which they were released. Relatively low aerosol concentration was observed in the corridor next to the Class N rooms. However, this could still be a risk for the patients in the Class N rooms despite the low concentration given the negative pressure pumping aerosol-carrying air to flow into the Class N rooms. The results showed that a net particle flow rate of 5.5×10^{-14} kg/s flowed into the Class N rooms, which was 4% of the total particle mass flow rate into the common area.

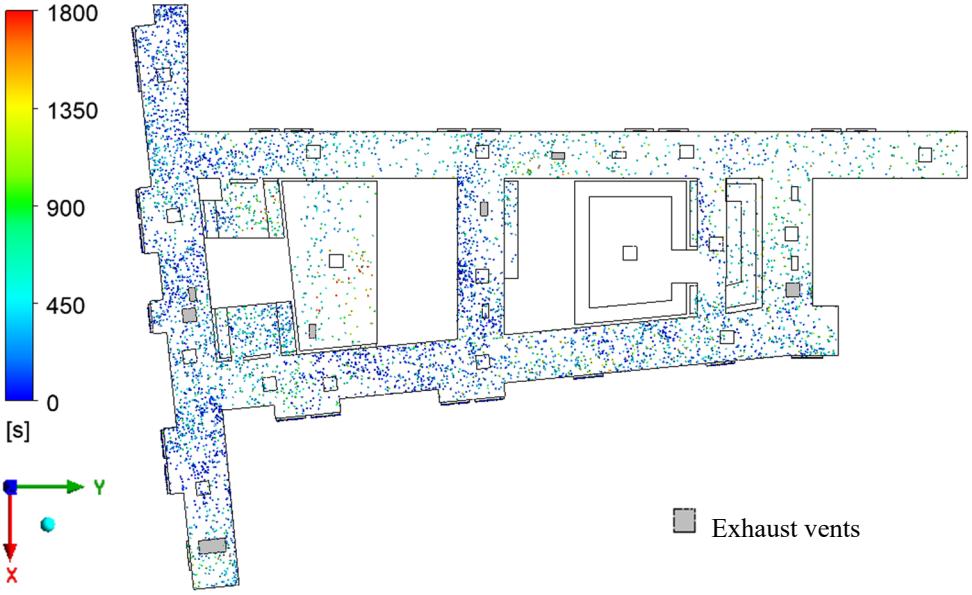

Figure 3. Particles distribution pattern in the domain.

We observed that the particles entering the corridors via the door gaps had different movement trajectories depending on the height of injection, as shown in Figure 4. The blue trajectories represented particles entering through the horizontal gaps close to the floor, while red trajectories represented particles emanating from the vertical gap. Particles flowing through the horizontal door gap and those through the lower part of the vertical gap were less affected by the directional air flow in the corridor because they sit in, or close to, the boundary layer, which allowed them to move following the floor surface until they reached the opposite wall. Some of the particles settled on the wall upon collision with the wall, while some others were gradually picked up by the directional airflow. On the contrary, the movement of most particles flowing through the vertical gaps were quickly entrained into the bulk airflow in the corridor. Thus, strategic positioning of door gaps, seals, or grilles could be used to preferentially manipulate trajectories of infectious particles emanating from patient rooms.

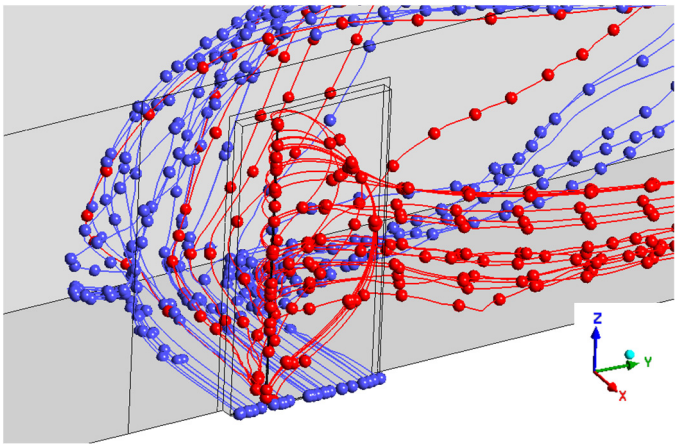

Figure 4. Particles entering the common area through horizontal gaps next to the floor have very different trajectories than those entering through the vertical gaps.

Figure 5 shows the particle deposition pattern on the ward surfaces, including the floor, nurse stations, and work room walls. The walls of the Class S rooms are omitted from the figure for clarity. The particle deposition rate was normalised according to the particle mass flux at the door gaps. The results showed that 37% of the injected particles were deposited on solid surfaces in the ward. Although the "no-bounce" assumption might have led to overprediction of the particle deposition rate, the simulations generated important information for the identification of key areas of surface contamination, thus were helpful for improving environment sanitation and reducing fomite transmission. The settled particles could be a source of fomite transmission of HAIs [34] and contribute to enhanced airborne transmission if they resuspended from the surfaces [35]. Although these transmission mechanisms were not discussed in the current study, the simulated particle deposition could provide useful information for relevant studies. As shown in the figure, particle deposition mainly happened on the floor immediately in front of and on the walls opposite to the doors of the Class S rooms, suggesting that inertial particle impact was a major source of surface contamination given the relatively high-speed jet flows from the door gaps (Figure 4).

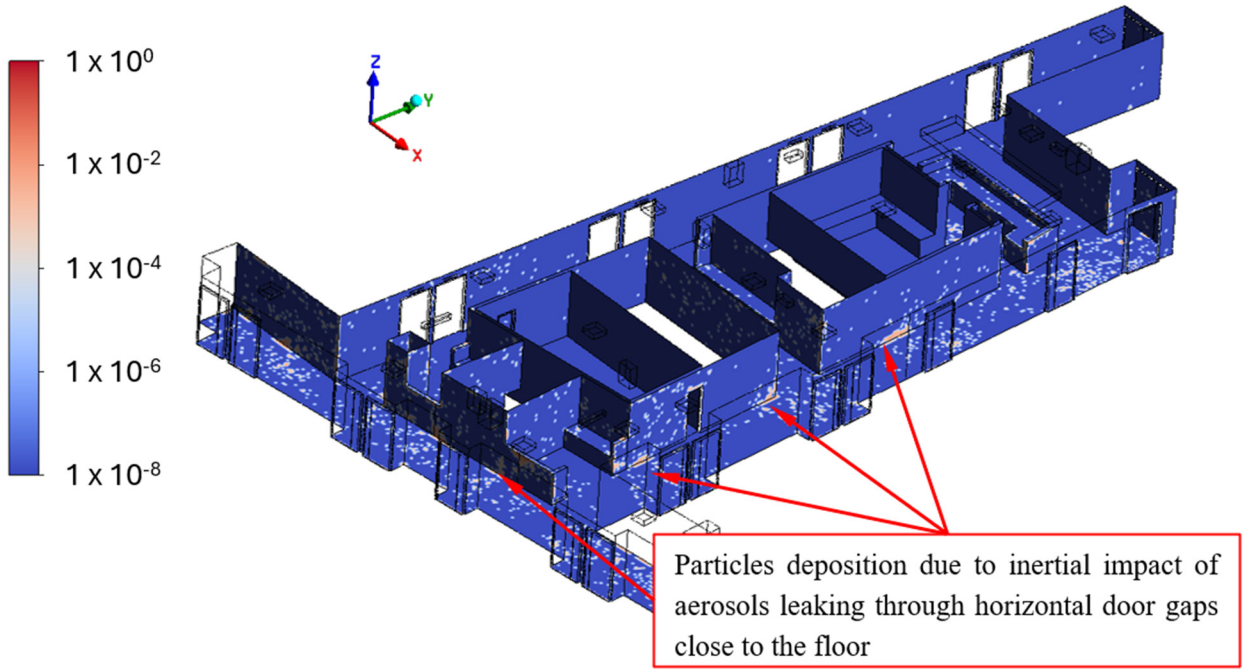

Figure 5. Distribution of the normalised particle deposition rate on the floor and walls. *Note: The particle deposition flux was normalised according to the particle mass flux at the releasing door* gaps.

2.2. Assessment of Airborne Transmission Risk in the Ward

In order to assess the transmission risk of airborne infection in the investigated common area, the spatially resolved dose-response model for the evaluation of airborne infections developed by Li et al. [29] was employed. The pathological and clinical data of COVID-19 reported in the literature was used as an example to evaluate the transmissibility of a specific disease. The model comprehensively considered an array of factors affecting the outcome of an exposure to virus-laden aerosols, and expressed the infection probability in a 3D space as

$$P(\boldsymbol{x}) = 1 - exp\left(-(1-\eta_S)\frac{ln2}{HID_{50}}\frac{c(\boldsymbol{x})d_{p,0}^3}{d_p^3}C_{virion}pt_e\right) \quad (1)$$

where $P(\boldsymbol{x})$ is the infection probably at spatial position $\boldsymbol{x}$, and η_S is the filtration efficiency of the PPE worn by the susceptible population. It was assumed that all occupants in the common area wore N95 respirators (η_S = 0.98 [36]), consistent with protocols that were in place during the height of the COVID-19 pandemic. The local volume fraction of virus-laden particles $c(\boldsymbol{x})$ was obtained based on the Lagrangian particle trajectories (Figure 3) using the so-called particle source in cell (PSIC) method [37]. The variables $d_{p,0}$ and d_p are the diameters of hydrated respiratory droplets and desiccated droplet nuclei, respectively. In this study, d_p = 0.262 $d_{p,0}$ is assumed according to a previous calculation [37]; p is the pulmonary ventilation rate, where p = 6 L/min is used in this study, representing the inhalation rate of a normal person under the rest condition [38]; and t_e is the exposure time, where t_e = 28,800 s is used in this study, representing an 8 h work shift. The spontaneous decay of virus was not considered in the model because the half-life of SARS-CoV-2 was reported to be 3 h [39], which is very long compared to 10 to 15 min mean particle residence time in most indoor spaces.

Key parameters in Equation (1) included the concentration of active infectious viruses (or virions) in the respiratory liquid of the infected person C_{virion}, and the median human infectious dose HID50, which was the dose of virions needed to infect 50% of the susceptible

population. SARS-CoV-2 is a type of highly contagious virus, with the HID50 value between 100 and 1000 virions [40] depending on the variant of virus and immunisation level of the susceptible population. This study adopted the median value of HID50 = 500 virions as recommended by Gale [41]. The virion concentration C_{virion} was estimated from the mean ribonucleic acid (RNA) concentration (known as the viral load) measured using the reverse transcription–polymerase chain reaction (RT-PCR) technique [42]. However, it should be noted that this may overpredict the infection probability as an RNA copy is not always associated with an infectious virion.

The infection probability of COVID-19 in the ward was calculated based on the simulated aerosol concentration field and using different values of viral load, as shown in Figure 6. The results showed that the viral load in exhaled respiratory particles was a strong factor influencing the infection probability. With a low viral load (7.99×10^4 RNA copies/mL [42]), the infection probability was close to zero throughout the domain with the maximum value smaller than 0.001 (Figure 6a). In this case, N95 respirators ($\eta_S = 0.98$) could provide very good protections. However, with a high viral load (1.3×10^8 RNA copies/mL [43]), significant infection probabilities were predicted, with the maximum infection probability of an 8 h exposure exceeding 0.70, even if N95 respirators were worn (Figure 6b).

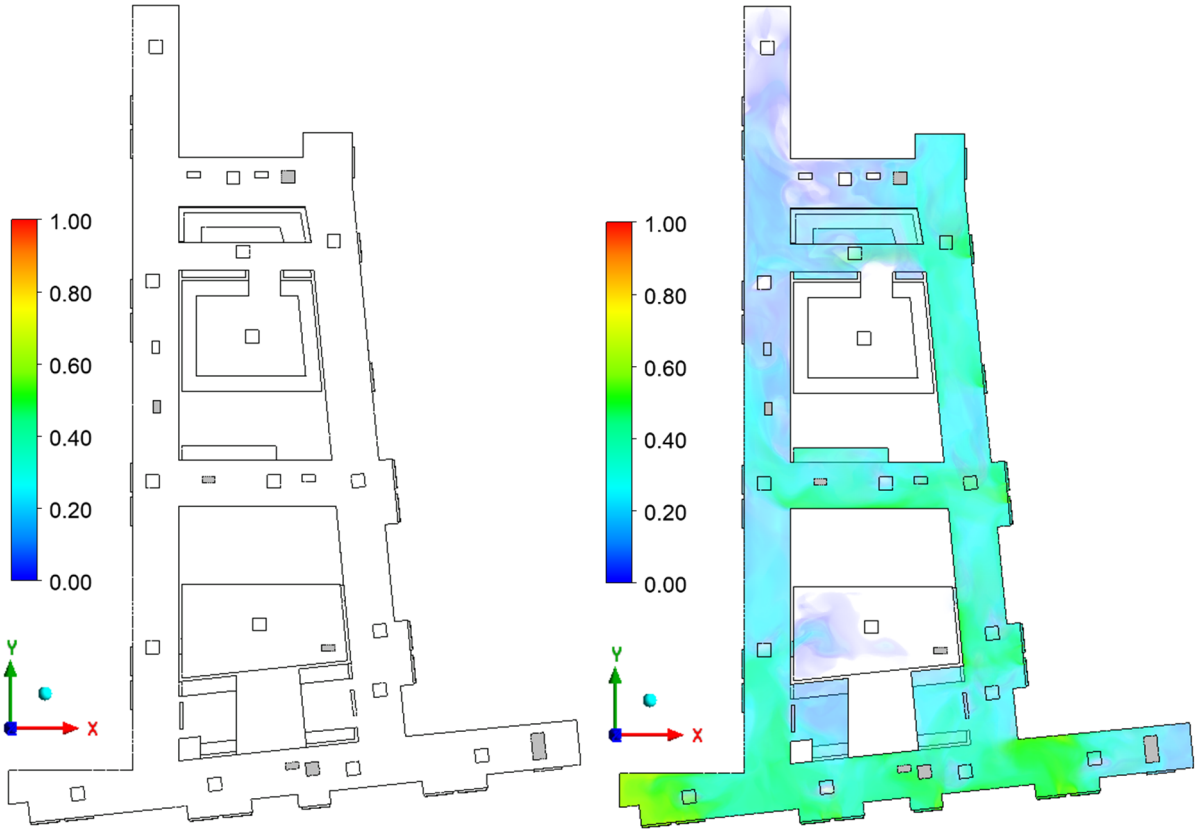

(**a**) C_{virion} = 7.99 × 10⁴ RNA copies/mL (**b**) C_{virion} = 1.26 × 10⁸ RNA copies/mL

Figure 6. Effects of viral load on infection probability in the ward (8 h exposure, N95 respirators in use).

For generality and to eliminate the uncertainties due to the use of RNA data, the infection probability was normalised using the local infection probability at the door gaps, which represented the maximum infection probability in the domain under various conditions, as shown in Figure 7. The normalised infection probability represented the relative infection risk in the common area compared to that in the patient rooms. The

results showed that the spatial distribution of the transmission risk was highly uneven, with the corridors next to the Class S rooms having higher infection risks than other regions. The highest infection probability appeared in the regions immediately next to the leaking door gaps. The risk decreased as the aerosols were diluted when they moved away from the door gaps. The infection probability remained high in some local regions with poor ventilation, such as the low-X corridor end.

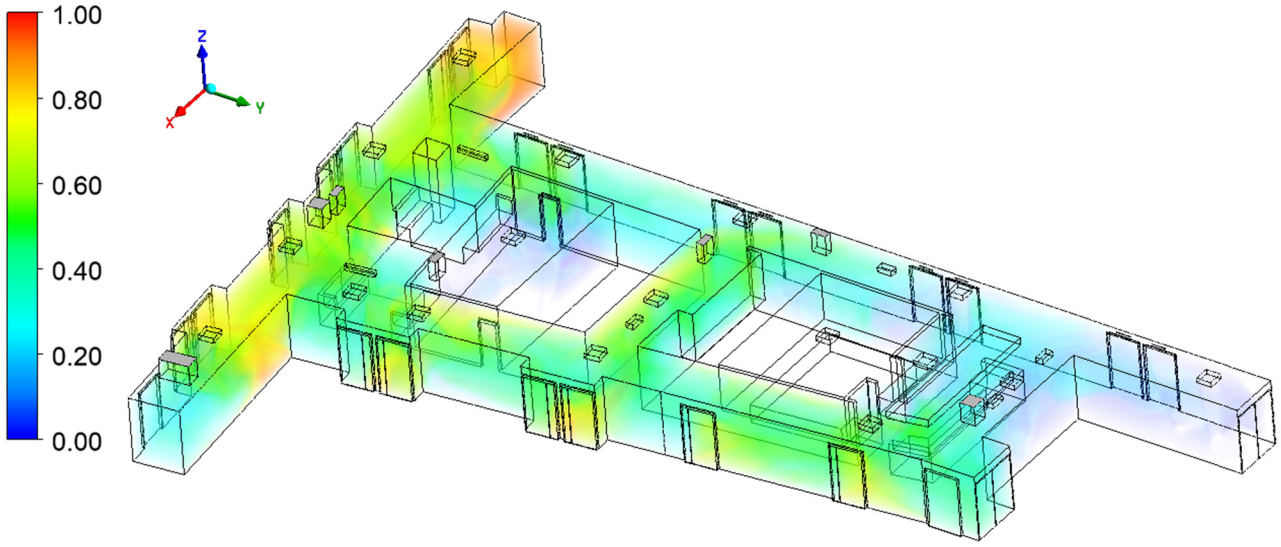

Figure 7. Volume rendering of the normalised infection probability of COVID-19 in the ward.

The simulations showed that high aerosol concentrations, and thus high infection probabilities, mainly existed in regions close to the source of contamination; namely, in the corridors next to the Class S rooms. Unfortunately, there were only a few exhaust vents installed in these corridors, which hindered fast removal of virus-laden aerosols. In addition, the directional air flow along the corridors contributed to the dispersion and long-distance transport of the aerosols. It was therefore believed that there was room for improvement of the current ventilation design in order to achieve more effective protections against airborne HAIs.

3. Improving Ventilation Design to Mitigate HAIs

Many studies [24,44] have proven that placing the exhaust vent close to the source of aerosols could be an effective approach to reduce aerosol dispersion, as the out-flowing air can help remove the particles. We applied this principle here to mitigate airborne transmission by optimising the placement of the HVAC vents, as detailed below.

The main features of ventilation improvement included the following:

- Exhaust vents were placed immediately next to the doors of all patient rooms, which resulted in an increased number of exhaust vents compared to the current setup.
- Supply and exhaust vents were installed alternately along the corridors. This setup was hoped to reduce the directional air flow and long-distance transport of aerosols.
- The supply rate was equal across all supply vents and a uniform discharge pressure was applied at all exhaust vents.
- The total air supply rate via the supply vents and air leak rate via door gaps remained unchanged (totally 8.1 ACH) for comparability against the current setup.

The distribution of ceiling vents in the improved configuration is shown in Figure 8. The current vent distribution is also included in the figure for comparison. In addition to the carefully determined locations of vents, a key change was that the improved ventilation

design had fewer supply vents (18 vs. 23) but more exhaust vents (14 vs. 7) than the current configuration.

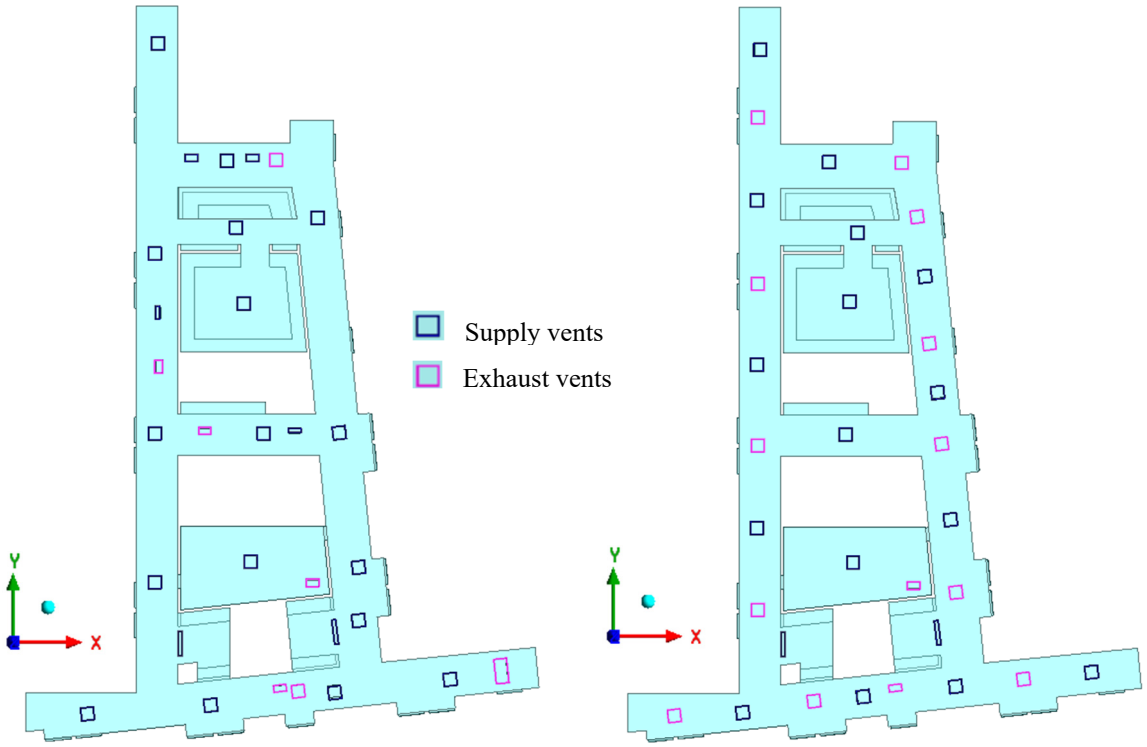

(**a**) Current vents distribution (**b**) Improved vents distribution

Figure 8. Ventilation optimisation of the ward common area.

The trajectories of particles entering the corridor from six selected Class S rooms are shown in Figure 9. A total of 130,000 particles were tracked in the simulations; however, only 60 representative particle trajectories (10 from each selected room) are shown in the figure for the sake of clarity. Particles from different rooms are marked with different colours. The simulations showed that under the current ventilation design (Figure 9a), particles from different rooms had very different trajectory features. Particles from the high-X rooms (S01 to S06) were strongly affected by the directional airflow, while most of those from the low-Y rooms (S07 to S13) were locked in the corridor. With the improved ventilation design (Figure 9b), there was very little long-distance particle transport due to the reduced directional air flow. Most particles were discharged via the nearest exhaust vents. However, it is noted that particles from Room S03 (red trajectories) still travelled transversely towards the Class N rooms due to the existence of a transverse corridor connecting two longitudinal corridors. Therefore, the corridor geometry was deemed as another factor strongly affecting aerosol transport.

The mean residence time of particles from different rooms are presented in Figure 10a. The results showed that with the current ventilation design, particles from standard pressure rooms S01–S04 had a relatively short residence time (between 124 s and 188 s) due to the directional air flow. In contrast, those from rooms S05–S13 had a longer residence time (between 207 s and 335 s) due to the lack of exhaust vents in the low-Y corridor. With the improved ventilation design, particles from most rooms had mean residence times between 184 s and 234 s. Although the residence times of particles from rooms S01–S04 slightly increased due to the reduced directional air flow, particles from other rooms had clearly shorter residence times due to the improved air exhaust. A close examination of rooms S01 and S03 revealed that they faced a nurse station and transverse corridor, respectively;

therefore, particles from those rooms had the chance to disperse transversely, resulting in longer-distance dispersion. Compared with the current ventilation system, the overall mean particle residence time under the optimised ventilation design decreased from 240 s down to 213 s, equivalent to an 11% reduction.

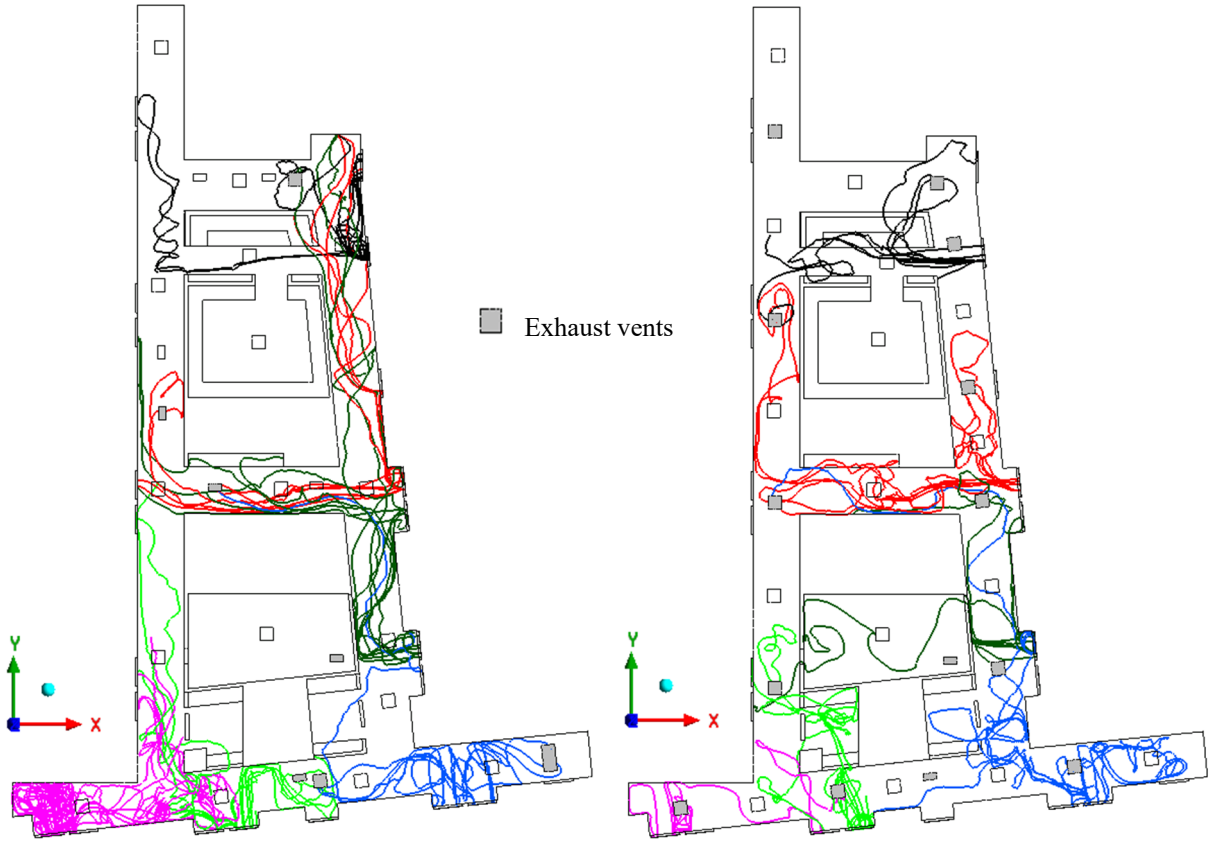

(**a**) Current ventilation setup (**b**) Optimised ventilation setup

Figure 9. Representative particle trajectories from selected Class S rooms. *Note: particles released from different rooms are marked with different colours*.

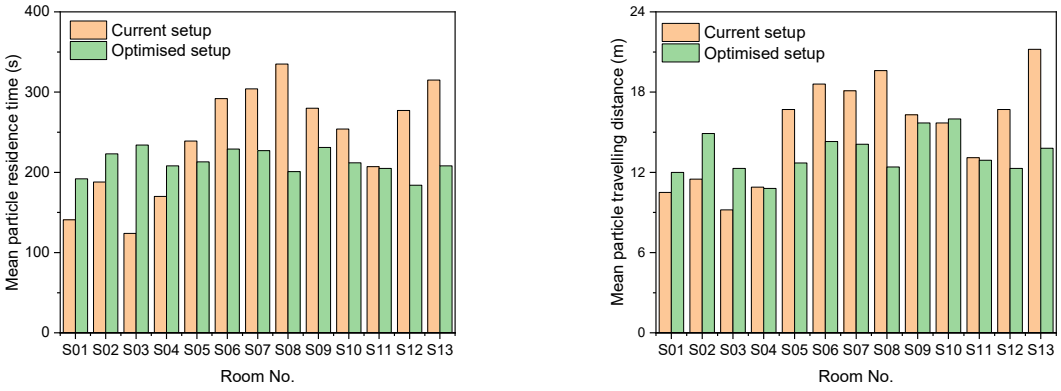

(**a**) Mean particle residence time (**b**) Mean particle travelling distance

Figure 10. Mean residence time and travelling distance of particles released from different rooms.

Correspondingly, the mean particle travelling distances are shown in Figure 10b. Here, the particle travelling distance was defined as the distance over which particles had travelled before they were discharged via the exhaust vents or settled on solid surfaces. The results showed that after the ventilation improvement, the travelling distance of

particles from rooms S01–S03 slightly increased due to the reduced directional air flow, while particles from most rooms had a short mean travelling distance. The mean travelling distance of all particles decreased from 15.2 m down to 13.7 m, equivalent to a 10% reduction. This decrease was mainly due to the fast removal of particles via the nearest exhaust vents soon after they entered the corridor. Overall, reduced particle residence time and travelling distance were achieved in most of the common area, which would contribute to lower levels of aerosol exposure.

The normalised infection probability was calculated and plotted in Figure 11. The infection probability was divided into three bands: low-risk zone ($p \leq 0.25$, green zone), medium-risk zone ($0.25 < p < 0.75$, yellow zone), and high-risk zone ($p \geq 0.75$, red zone). The corresponding area fractions of each zone relative to the area of the breathing plane (Z = 1.2 m) are listed in Table 2. The results showed that re-arrangement of HVAC vents clearly reduced the overall transmission risk within the ward. With the current ventilation system, the area fraction of the green zone ($p \leq 0.25$) was 0.402 while over half of the ward was in the medium-risk zone (area fraction 0.567), as shown in Figure 11a. In particular, a substantial part of the corridor next to the Class N rooms had an infection probability exceeding 0.25, which might be problematic for the patients isolated in the Class N rooms due to their vulnerability and the negative pressure pumping virus-laden aerosols into the rooms. With the improved ventilation design, the area fraction of the green zone was significantly improved. As shown in Figure 11b, the green zone ($p \leq 0.25$) covered almost the entire corridor next to the Class N rooms and had an overall area fraction of 0.555, which was a 38% improvement. The area fraction of the yellow zone ($0.25 < p < 0.75$) decreased from 0.567 to 0.429 with the improved ventilation design. In both cases, the red high-risk zones ($p \geq 0.75$) were mainly located in the vicinity of the doors of the Class S rooms. The ventilation improvement reduced the area fraction of the red zone from 0.031 down to 0.016, a reduction of 48%. The overall mean infection probability decreased from 0.320 to 0.260, a reduction of 19%.

Table 2. Areas with different levels of infection probability in the plane Z = 1.2 m.

	Area Fraction of Different Risk Zones			**Average Infection Probability**
	$p \leq 0.25$	$0.25 < p < 0.75$	$p \geq 0.75$	
Current	0.402	0.567	0.031	0.320
Optimised	0.555	0.429	0.016	0.260

This study demonstrated that a small change in the layout of the supply and exhaust vents could contribute to much reduced transmission risks in the ward. The key to the improvement was the more evenly distributed air supply and exhaust vents preventing directional air flow along the corridor, in addition to the exhaust vents being placed close to the source of aerosols. However, we noted that almost half of the breathing plane was still medium- or high-risk zones even after the ventilation improvement (Figure 11b). The main reason was that there were continuous injections of virus-laden particles from the Class S rooms into the corridor. To reduce the infection risk in the common area, controlling the aerosol source is critical and this can be achieved via adding room-return exhausts in the patient rooms or using personal exhaust devices such as the McMonty hood [45] developed by the authors. In addition, the optimised ventilation design of this study still featured a mixing ventilation scheme, which served to dilute contaminants through air mixing. This would inevitably enhance aerosol dispersion and hinder aerosol removal. It is expected that reduced air mixing or using an up-rising air flow pattern would be more efficient in preventing aerosol dispersion and rapidly removing aerosols. From this perspective,

displacement ventilation or under floor air distribution systems may be more beneficial for the prevention of airborne HAIs.

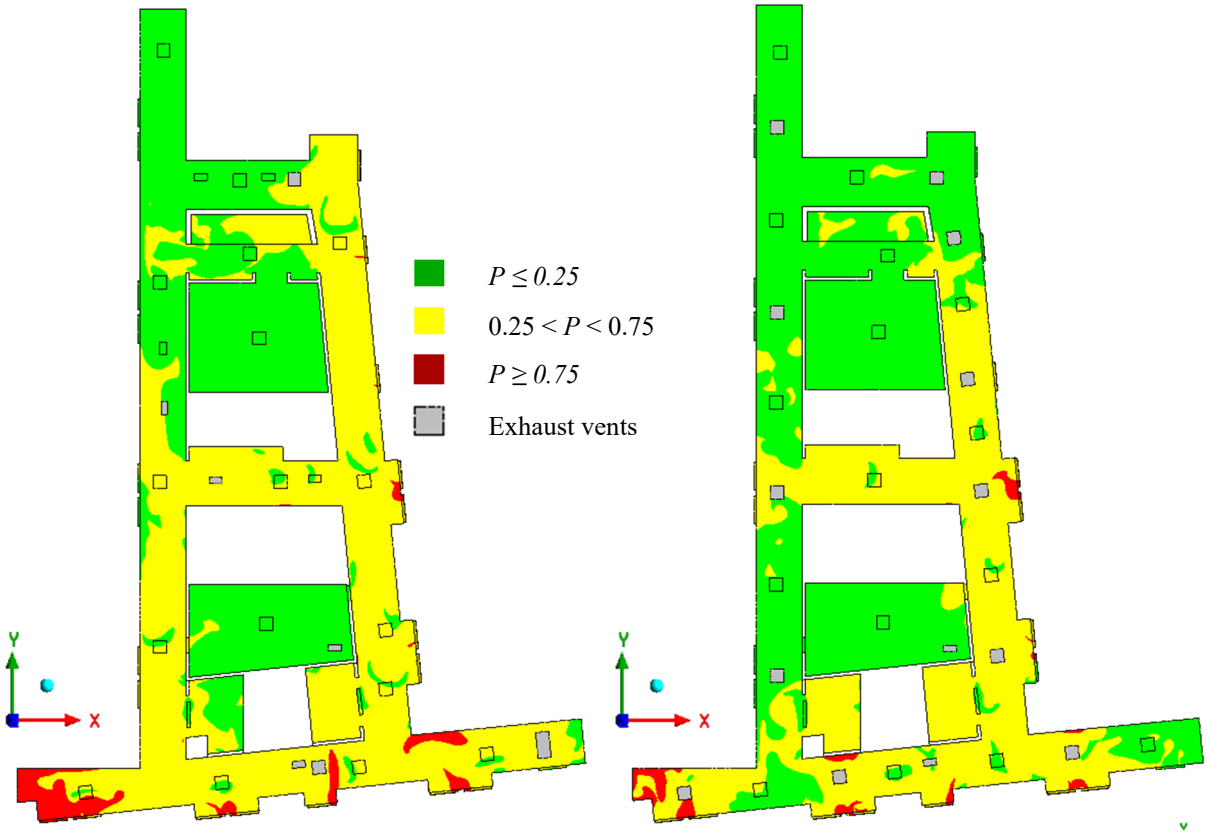

(**a**) Current ventilation setup (**b**) Optimised ventilation setup

Figure 11. Distribution of risk bands at Z = 1.2 m.

4. Conclusions

Using multiphase computational fluid dynamics, we analysed the air flow field and aerosol transport in the common areas of an inpatient ward equipped with a mixing ventilation system. A spatially resolved infection risk model was employed to evaluate the airborne transmission in the ward. Conclusions rising from this study are as follows:

(1) The central-return mixing ventilation system created directional air flows in the corridors, which contributed to enhanced air mixing and long-distance transport of aerosols while leaving high aerosol concentration in local regions with poor ventilation. When the ward had different types of patient rooms with different operating pressures, the aerosols escaping from the standard- or positive pressure rooms may have the chance to transport into the negative pressure rooms via the common area if these rooms were not properly configured.

(2) This study highlighted the importance of properly positioning supply and exhaust vents. By placing the exhaust vents close to the sources of aerosol release and applying an even air flow rate across the supply vents, the improved ventilation design reduced the directional air flows and facilitated aerosol discharge, reducing transmission risks throughout the ward. With the improved ventilation system, the area of the low-risk zone in the ward increased by 38% compared to the existing ventilation system, while the mean relative infection probability dropped from 0.320 to 0.260, equivalent to a 19% reduction.

This study demonstrated the importance of preventing long-distance air flow and reducing air mixing in order to reduce aerosol concentration in the ward. The improved vent layout we described effectively reduces the concentration levels by minimising directional air flow. However, with a mixing ventilation system, the size of the medium- and high-risk zones was still remarkable even after the improvements. Our findings suggested that to further reduce air mixing, the displacement ventilation or under floor air distribution schemes that create an uprising air flow pattern may be a promising target for additional design improvements.

Author Contributions: Conceptualization, X.L., K.K., W.K.L., A.O. and J.M.; methodology, X.L., W.K.L., A.O. and J.M.; software, L.T.; validation, X.L. and W.K.L.; formal analysis, X.L. and K.K.; investigation, C.Z. and N.G.; resources, S.B., F.M. and M.K.; data curation, L.T., C.Z. and N.G.; writing—original draft preparation, X.L. and L.T.; writing—review and editing, All authors; visualization, X.L., K.K., W.K.L. and A.O.; supervision, J.M. and L.M.; project administration, K.K. and L.T.; funding acquisition, J.M., M.K. and L.M. All authors have read and agreed to the published version of the manuscript.

Funding: This study is supported by the Australian Research Council via the ARC Training Centre for Advanced Building Systems against Airborne Infection Transmission (IC220100012), Medical Research Future Fund (MRF2017355), and the National Health and Medical Research Council (Project ID 2044089).

Institutional Review Board Statement: Not applicable.

Informed Consent Statement: Not applicable.

Data Availability Statement: Dataset available on request from the authors.

Conflicts of Interest: The authors declare no conflicts of interest.

References

1. Lydeamore, M.J.; Mitchell, B.G.; Bucknall, T.; Cheng, A.C.; Russo, P.L.; Stewardson, A.J. Burden of five healthcare associted infections in Australia. *Antimicrob Resist. Infect Control* **2022**, *11*, 69. [CrossRef] [PubMed]
2. Australian Commission on Safety and Quality in Health. *National Safety and Quality Health Service Standards*, 2nd ed.; NSW: Sydney, Australia, 2000.
3. WHO. *Global Technical Consultation Report on Proposed Terminology for Pathogens That Transmit Through the Air*; WHO: Geneva, Switzerland, 2024.
4. Wong, B.C.K.; Lee, N.; Li, Y.; Chan, P.K.S.; Qiu, H.; Luo, Z.; Lai, R.W.M.; Ngai, K.L.K.; Hui, D.S.C.; Choi, K.W.; et al. Possible role of aerosol transmission in a hospital outbreak of influenza. *Clin. Infect. Dis.* **2010**, *51*, 1176–1183. [CrossRef] [PubMed]
5. Watkins, N.M.; Smith, R.P.; Germain, D.L.S.; MacKay, D.N. Measles (rubeola) infection in a hospital setting. *Am. J. Infect. Control* **1987**, *15*, 201–206. [CrossRef]
6. Griffith, D.E.; Hardeman, J.L.; Zhang, Y.; Wallace, R.J.; Mazurek, G.H. Tuberculosis outbreak among healthcare workers in a community hospital. *Am. J. Respir. Crit. Care Med.* **1995**, *152*, 808–811. [CrossRef]
7. Sarit, S.; Shruti, S.; Deepinder, C.; Chhina, R.S. Chicken pox outbreak in the Intensive Care Unit of a tertiary care hospital: Lessons learnt the hard way. *Indian J. Crit. Care Med.* **2015**, *19*, 723–725. [CrossRef]
8. Dwosh, H.A.; Hong, H.H.L.; Austgarden, D.; Herman, S.; Schabas, R. Identification and containment of an outbreak of SARS in a community hospital. *CMAJ* **2003**, *168*, 1415–1420.
9. Xiao, S.; Li, Y.; Sung, M.; Wei, J.; Yang, Z. A study of the probable transmission routes of MERS-CoV during the first hospital outbreak in the Republic of Korea. *Indoor Air* **2018**, *28*, 51–63. [CrossRef] [PubMed]
10. Ciccacci, F.; De Santo, C.; Mosconi, C.; Orlando, S.; Carestia, M.; Guarente, L.; Liotta, G.; Palombi, L.; Gialloreti, L.E. Not only COVID-19: A systematic review of anti-COVID-19 measures and their effect on healthcare-associated infections. *J. Hosp. Infect.* **2024**, *147*, 133–145. [CrossRef]
11. Quigley, A.L.; Stone, H.; Nguyen, P.Y.; Chughtai, A.A.; MacIntyre, C.R. Estimating the burden of COVID-19 on the Australian healthcare workers and health system during the first six months of the pandemic. *Int. J. Nurs. Stud.* **2021**, *114*, 103811. [CrossRef]
12. McGain, F.; Burnham, J.P.; Lau, R.; Aye, L.; Kollef, M.H.; McAlister, S. The carbon footprint of treating patients with septic shock in the intensive care unit. *Crit. Care Resusc.* **2018**, *20*, 304–312. [CrossRef]

13. Bloch, N.; Rüfenacht, S.; Ludwinek, M.; Frick, W.; Kleger, G.-R.; Schneider, F.; Albrich, W.C.; Flury, D.; Kuster, S.P.; Schlegel, M.; et al. Healthcare-associated infections in intensive care unit patients with and without COVID-19: A single center prospective surveillance study. *Antimicrob. Resist. Infect. Control* **2023**, *12*, 147. [CrossRef] [PubMed]
14. Lawton, T.; Butler, M.; Peters, C. Airborne protection for staff is associated with reduced hospital-acquired COVID-19 in English NHS trusts. *J. Hosp. Infect.* **2022**, *120*, 81–84. [CrossRef] [PubMed]
15. Skidmore, G.; Monty, J.; Kevin, K. *Ventilation Assessment for Infection Control—Sunshine Hospital Inpatient Ward 3F*; The University of Melbourne: Melbourne, Australia, 2020.
16. Victorian Health Building Authority. *Engineering Guidelines for Healthcare Facilities: Volume 4—Heating, Ventilation and Air Conditioning*; Victorian Health Building Authority: Melbourne, Australia, 2020.
17. McGain, F.; Wickramarachchi, K.; Aye, L.; Chan, B.G.; Sheridan, N.; Tran, P.; McAlister, S. The carbon footprint of total knee replacements. *Aust. Health Rev.* **2024**, *48*, 664–672. [CrossRef]
18. Singh, R.; Zia, H.; Seth, M.; Ahmed, A.; Azim, A. Engineering Solutions for Preventing Airborne Transmission in Hospitals with Resource Limitation and Demand Surge. *Indian J. Crit. Care Med.* **2021**, *25*, 453–460. [CrossRef]
19. Morawska, L.; Johnson, G.R.; Ristovski, Z.D.; Hargreaves, M.; Mengersen, K.; Corbett, S.; Chao, C.Y.H.; Li, Y.; Katoshevski, D. Size distribution and sites of origin of droplets expelled from the human respiratory tract during expiratory activities. *J. Aerosol. Sci.* **2009**, *40*, 256–269. [CrossRef]
20. Seelye, A. Hospital ward layout and nurse staffing. *J. Adv. Nurs.* **1982**, *7*, 195–201. [CrossRef]
21. Nourozi, B.; Wierzbicka, A.; Yao, R.; Sadrizadeh, S. A systematic review of ventilation solutions for hospital wards: Addressing cross-infection and patient safety. *Build. Environ.* **2024**, *247*, 110954.
22. Sadrizadeh, S.; Aganovic, A.; Bogdan, A.; Wang, C.; Afshari, A.; Hartmann, A.; Croitoru, C.; Khan, A.; Kriegel, M.; Lind, M.; et al. A systematic review of operating room ventilation. *J. Build. Eng.* **2021**, *40*, 102693. [CrossRef]
23. King, K.G.; Delclos, G.L.; Brown, E.L.; Emery, S.T.; Yamal, J.M.; Emery, R.J. An assessment of outpatient clinic room ventilation systems and possible relationship to disease transmission. *Am. J. Infect. Control* **2021**, *49*, 808–812. [CrossRef] [PubMed]
24. Kaeophet, T.; Dejchanchaiwong, R.; Tekasakul, P.; Phonsahwat, T.; Khongprom, P.; Ingviya, T.; Kongkamol, C.; Morris, J. Ventilation improvement for effective protection of healthcare workers in negative pressure airborne infectious isolation room from viral aerosols. *Build. Environ.* **2024**, *259*, 111665. [CrossRef]
25. Zheng, M.; Fan, Y.; Li, X.; Lester, D.; Chen, X.; Li, Y.; Cole, I. Aerosol exchange between pressure-equilibrium rooms induced by door motion and human movement. *Build. Environ.* **2023**, *241*, 110486. [CrossRef]
26. Westbrook, J.I.; Duffield, C.; Li, L.; Creswick, N.J. How much time do nurses have for patients? A longitudinal study quantifying hospital nurses' patterns of task time distribution and interactions with health professionals. *BMC Health Serv. Res.* **2011**, *11*, 319. [CrossRef] [PubMed]
27. Walsby, A.; Williams, S.; Gammon, J.; Best, S. The reality of nursing time: How nurses spend their shifts. *Br. J. Nurs.* **2024**, *33*, 968–974. [CrossRef]
28. Cheng, P.; Chen, W.; Xiao, S.; Xue, F.; Wang, Q.; Chan, P.W.; You, R.; Lin, Z.; Niu, J.; Li, Y. Probable cross-corridor transmission of SARS-CoV-2 due to cross airflows and its control. *Build. Environ.* **2022**, *218*, 109137. [CrossRef]
29. Li, X.D.; Lester, D.; Rosengarten, G.; Aboltins, C.; Patel, M.; Cole, I. A spatiotemporally resolved infection risk model for airborne transmission of COVID-19 variants in indoor spaces. *Sci. Total Environ.* **2022**, *812*, 152592.
30. Li, X.; Yan, Y.; Shang, Y.; Tu, J. An Eulerian–Eulerian model for particulate matter transport in indoor spaces. *Build. Environ.* **2015**, *86*, 191–202. [CrossRef]
31. Li, X.; Tu, J. Evaluation of the eddy viscosity turbulence models for the simulation of convection–radiation coupled heat transfer in indoor environment. *Energy Build.* **2019**, *184*, 8–18. [CrossRef]
32. *ANSI/ASHRAE Standard 62.1-2022*; Ventilation and Acceptable Indoor Air Quality. ASHRAE: Suburban Atlanta, GA USA, 2022.
33. Duval, D.; Palmer, J.C.; Tudge, I.; Pearce-Smith, N.; O'cOnnell, E.; Bennett, A.; Clark, R. Long distance airborne transmission of SARS-CoV-2: Rapid systematic review. *BMJ* **2022**, *377*, e068743. [CrossRef] [PubMed]
34. Short, K.R.; Cowling, B.J. Cowling, Assessing the potential for fomite transmission of SARS-CoV-2. *Lancet Microbe* **2023**, *4*, e380–e381.
35. Jhang, H.-Y.; Yang, S.; Licina, D. Resuspension of inhalable particles from clothing: A manikin-based chamber study. *Build. Environ.* **2025**, *267*, 112157. [CrossRef]
36. Clapp, P.W.; Sickbert-Bennett, E.E.; Samet, J.M.; Berntsen, J.; Zeman, K.L.; Anderson, D.J.; Weber, D.J.; Bennett, W.D. Evaluation of Cloth Masks and Modified Procedure Masks as Personal Protective Equipment for the Public During the COVID-19 Pandemic. *JAMA Intern. Med.* **2021**, *181*, 463–469. [CrossRef]
37. Zhang, Z.; Chen, Q. Comparison of the Eulerian and Lagrangian methods for predicting particle transport in enclosed spaces. *Atmos. Environ.* **2007**, *41*, 5236–5248. [CrossRef]
38. Carroll, R.G. (Ed.) *10—Pulmonary System, in Elsevier's Integrated Physiology*; Mosby: Philadelphia, PA, USA, 2007; pp. 99–115.

39. van Doremalen, N.; Bushmaker, T.; Morris, D.H.; Holbrook, M.G.; Gamble, A.; Williamson, B.N.; Tamin, A.; Harcourt, J.L.; Thornburg, N.J.; Gerber, S.I.; et al. Aerosol and Surface Stability of SARS-CoV-2 as Compared with SARS-CoV-1. *N. Engl. J. Med.* **2020**, *382*, 1564–1567. [CrossRef]
40. Prentiss, M.; Chu, A.; Berggren, K.K. Finding the infectious dose for COVID-19 by applying an airborne-transmission model to superspreader events. *PLoS ONE* **2022**, *17*, e0265816. [CrossRef]
41. Gale, P. Thermodynamic equilibrium dose-response models for MERS-CoV infection reveal a potential protective role of human lung mucus but not for SARS-CoV-2. *Microb. Risk Anal.* **2020**, *16*, 100140. [CrossRef]
42. Pan, Y.; Zhang, D.; Yang, P.; Poon, L.L.M.; Wang, Q. Viral load of SARS-CoV-2 in clinical samples. *Lancet Infect. Dis.* **2020**, *20*, 411–412. [CrossRef]
43. Costa, R.; Olea, B.; Bracho, M.A.; Albert, E.; de Michelena, P.; Martínez-Costa, C.; González-Candelas, F.; Navarro, D. RNA viral loads of SARS-CoV-2 Alpha and Delta variants in nasopharyngeal specimens at diagnosis stratified by age, clinical presentation and vaccination status. *J. Infect.* **2022**, *84*, 579–613. [CrossRef]
44. Almhafdy, A.; Korany, H.Z.; AlSaleem, S.S.; Cao, S.-J. Airflow distribution in hospital isolation rooms with different ventilation and exhaust vent configurations. *Indoor Built Environ.* **2024**, *33*, 23–37. [CrossRef]
45. McGain, F.; Humphries, R.S.; Lee, J.H.; Schofield, R.; French, C.; Keywood, M.D.; Irving, L.; Kevin, K.; Patel, J.; Monty, J. Aerosol generation related to respiratory interventions and the effectiveness of a personal ventilation hood. *Crit. Care Resusc.* **2020**, *22*, 212–220. [CrossRef]